PERGAMON

Journal of Structural Geology 22 (2000) 1199–1219

JOURNAL OF STRUCTURAL GEOLOGY

www.elsevier.nl/locate/jstrugeo

Preserved magnetic fabrics vs. annealed microstructures in the syntectonic recrystallised George granite, South Africa

E.C. Ferré[a], L. Améglio[a,b]

[a]*Department of Geology, Rhodes University, PO Box 94, Grahamstown 6140, South Africa*
[b]*Equipe de Pétrophysique, UMR 5563 CNRS, Université Paul Sabatier, 38 rue des 36 Ponts, 31400 Toulouse, France*

Received 2 October 1998; accepted 20 March 2000

Abstract

The Saldanian basement of the Cape Fold Belt of South Africa outcrops in the Kaaimans inlier with granite plutons intruded in low-grade pelitic and quartzitic metasediments around 535 Ma. New field data support a ubiquitous Saldanian top-to-the-north thrust kinematics coeval with granite emplacement with no substantial Cape tectonic overprint. The granites and their contact aureoles display both synkinematic and post-kinematic fabrics. This and the high strain zone commonly observed all along the contact between the Kaaimans inlier and the Cape Fold Belt, suggest a structural decoupling between the basement and its cover. Microstructures in the Kaaimans inlier and in the George pluton establish a post-kinematic, pervasive and thermal overprint of Saldanian age. Granites and country rocks record a medium-temperature/high-strain deformation phase followed by a strong low-temperature/static recrystallisation. Two sets of andalusite porphyroblasts occur systematically in the contact aureoles of the studied plutons and cannot be explained by successive magmatic pulses.

The granites, studied by the Anisotropy of Magnetic Susceptibility (AMS) technique, are paramagnetic ($20 < K_m < 300$ μSI). Biotite is mostly at the origin of the bulk rock susceptibility although minor contributions of tourmaline or ferromagnetic phases may occur. The contribution of biotite alone to the bulk magnetic susceptibility is supported by two quantitative models based, respectively, on whole rock compositions (Curie–Weiss law) and on intrinsic mineral susceptibilities. The magnetic foliations and lineations are homogeneous throughout the George pluton and are consistent with field structures. The AMS results mainly from the magneto-crystalline anisotropy of biotite and from its lattice preferred orientation (LPO) in the rock. The magnetic fabric reveals the biotite subfabrics that had been acquired before static recrystallisation and which was not modified by the subsequent thermal metamorphic event. The magnetic fabric therefore preserves the emplacement-related deformation fabric.

1. Introduction

The Anisotropy of Magnetic Susceptibility (AMS) technique is now a well-established fabric analysis tool in granitic rocks (e.g. Borradaile and Henry, 1997; Bouchez, 1997). AMS may be used under certain circumstances as a strain gauge (Borradaile, 1991) or as a method for the study of regional structural features (Archanjo et al., 1994; Ferré et al., 1995; Benn et al., 1997), this being particularly useful to decipher complex deformation histories (e.g. Benn et al., 1993; Bouchez and Gleizes, 1995; Ferré et al., 1997). This technique is commonly believed to provide structural insights on the latest increment of deformation in igneous intrusions (Paterson and Vernon, 1995) although no clear consensus exists on this issue (Saint Blanquat and Tikoff, 1997).

In a previous case study, Riller et al. (1996) reported the example of an AMS fabric in a granite pluton that was overprinted by a subsequent and much younger deformation phase. By contrast, our contribution investigates the effect of a tectono-thermal overprint, which occurred during and just after the emplacement

E-mail address: ferre@rock.ru.ac.za (E.C. Ferré).

0191-8141/00/$ - see front matter
PII: S0191-8141(00)00026-2

of a syntectonic pluton. The example presented here is from the late-Proterozoic basement of the Cape Fold Belt of South Africa.

2. Regional geology

The late Proterozoic Saldanian basement of South Africa (Fig. 1a) is unconformably overlain by the Palaeozoic Cape Fold Belt sediments (Söhnge and Hälbich, 1983). This basement consists of the 600–520-Ma-old Cape Granites intruded in greenschist-facies metasediments of the Malmesbury Group (Dunlevey, 1988, 1992; Hartnady et al., 1985). The Cape Granite Suite includes syn- to post-tectonic S-type, late-tectonic I-type and post-tectonic A-type intrusions (Scheepers, 1995). This basement is well exposed in the Cape Town area, although outcrops further east are limited to a few E–W elongated inliers (named Kaaimans, Gamtoos and Cango) exposed through the Cape Fold Belt cover (Gresse and Scheepers, 1993; Thomas et al., 1993). This contribution focuses on the Kaaimans inlier (Fig. 1b). The Cape Fold Belt sediments were deposited during the Ordovician to Devonian. They record an increasing metamorphism from north to south, from anchi- to epi-metamorphic facies (Söhnge and Hälbich, 1983; Gresse et al., 1992), coeval with folding and thrusting between 280 and 220 Ma. A very-low-temperature tectonic overprint occurred during the Cape orogeny near the margins of the Saldanian inlier. Half-grabens formed along inverted thrusts and were filled with Cretaceous and younger clastic sediments including conglomerates (Gresse et al., 1992).

The Kaaimans inlier crops out over 100 km E–W by 15 km N–S (Fig. 1b) and comprises low- to medium-grade metasediments referred to as the Kaaimans Group intruded by granitic plutons (Krynauw and Gresse, 1980; Krynauw, 1983; Gresse, 1983). The metasediments belong to seven formations dominated by quartzites, shales, phyllites, schists and calc-silicates with a total thickness of about 6000 m (Gresse, 1983; Frimmel and van Achterbergh, 1995). Graded bedding and cross-bedding structures indicate that these formations (Fig. 2), namely Silver River, Saasveld, Sandkraal, Skaapkops, Soetkraal, Victoria Bay and Homtini (to the far east), are in a normal way up position.

Four plutons, respectively named Great-Brak River, George, Woodville and Rooiklip, occur in the Kaaimans inlier (Fig. 1b). All are S-type syntectonic granites with high SiO_2 content (74%; Scheepers, 1995) and characterised by xenoliths of country rock and ellipsoidal mafic enclaves (up to 1 m in length). This study focuses on the George pluton (30 × 11 km) and

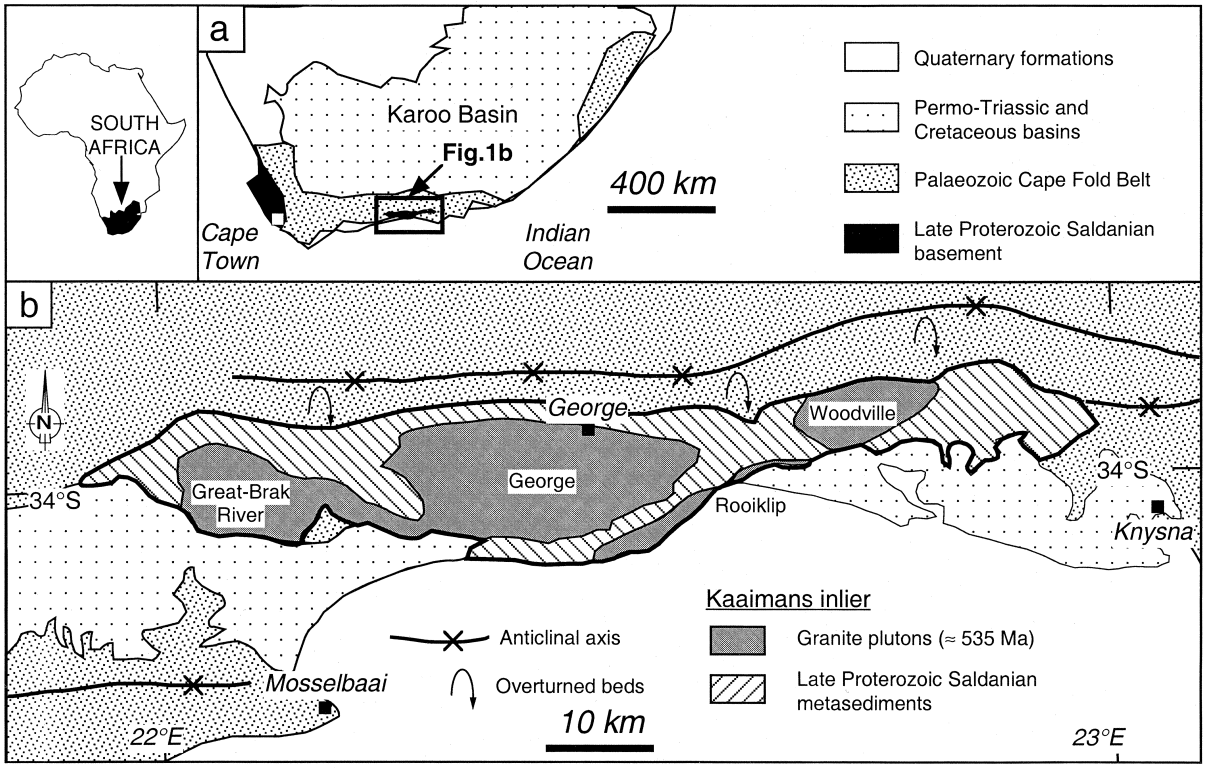

Fig. 1. Geological setting of the studied area. (a) Location of the Palaeozoic Cape Fold Belt and its Late Proterozoic Saldanian basement in South Africa (see inset). (b) Simplified map showing major geological and tectonic setting in the Kaaimans inlier.

the Rooiklip sill (25 × 1 km). The George pluton, dated at 535 ± 10 Ma from Pb evaporation of zircon (Scheepers, personal communication), has an elliptical outline and an east–west elongation (Fig. 1b). Three petrographic types have been distinguished within the George pluton (Fig. 2): the Maalgaten granite, the Kleinfontein leucogranite and the Modderkloof granodiorite. Mineral assemblages are listed in Table 1. In the following, mineral symbols are from Kretz (1983). The Maalgaten granite shows a coarse-grained matrix and Kfs megacrysts, up to 10 cm in length, with concentric zones of inclusions (Bt, Pl, Qtz) and albite rims. The Kleinfontein leucogranite forms a sheet-like body hosting a few ellipsoidal mafic enclaves (up to 35 cm in length) and cut by pegmatite dykes. The Modderkloof granodiorite is restricted to the eastern end of the George pluton. A few restitic zones, aplitic zones, and Grt–Ms-rich pegmatitic pockets occur along the northern margin of the George pluton. Numerous pegmatitic dykes cut through the George pluton and display the same mineral assemblage as the Maalgaten granite. The Rooiklip granite forms a slightly discordant sill (maximum thickness ca 600 m) of mostly aphyric, coarse-grained granite with a few miarolitic cavities, pegmatite veins and fluorite. Stable isotope data suggest that no significant hydrothermal alteration has affected the George and Rooiklip granites (Harris et al., 1997).

Contact metamorphism around the plutons occurred concomitantly with regional deformation as shown by the syn-kinematic growth of andalusite, biotite, muscovite and chloritoid (Krynauw, 1983; Gresse, 1983). Contact metamorphic conditions are characterised by high temperature–low pressure assemblages (450°C, 2.5 kbar; Frimmel and van Achterbergh, 1995). Large andalusite porphyroblasts (up to 80 × 25 mm^2) are a distinctive feature of the Saasveld Formation and occur in an aureole of about 300-m-thick around the George pluton. Similar but smaller in size aureoles occur around the Great Brak River and Woodville plutons. Staurolite occasionally forms euhedral leucoxene–Py–Chl pseudomorphic aggregates. Small elongate Chl–Ms clusters are parallel to the schistosity in the granite aureole in the Sandkraal Formation and are interpreted as synkinematic porphyroblasts. The Skaapkops Formation often displays a Pl–Ms–Qtz–Czo/Zo–Chl–Hem mineral assemblage. Qtz–Chl–Ms–

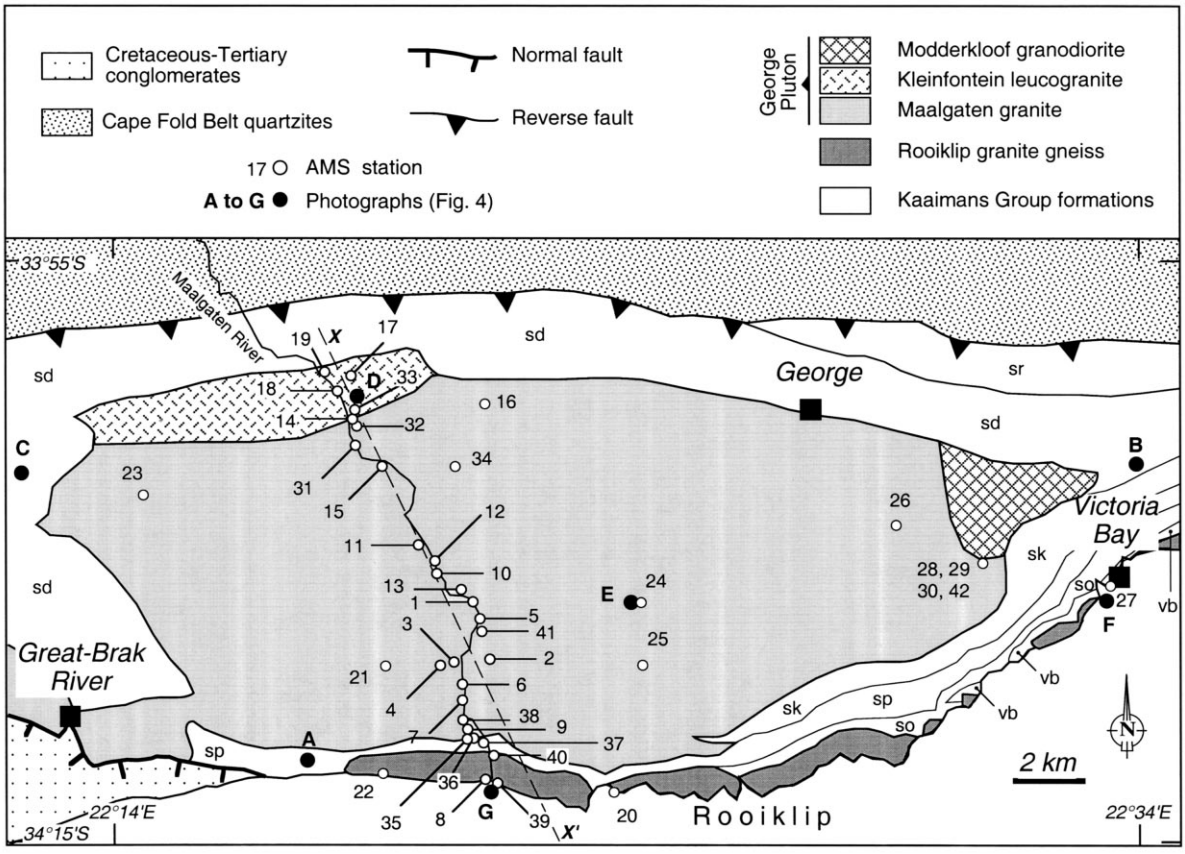

Fig. 2. Simplified geological map of the George area. Kaaimans Group formations: vb—Victoria Bay calc-silicates; so—Soetkraal schists; sp—Skaapkops quartzo-feldspathic schists; sk—Sandkraal quartzites; sd—Saasveld schists and sr—Silver River schists. Numbers refer to AMS stations (see Table 1). *XX′*: profile along the Maalgaten River of magnetic susceptibility data (see Fig. 6).

Table 1
Magnetic and field data of the George pluton[a]

		Magnetic data										Field data		GPS positioning					
														X			*Y*		
Station N°	Rock type	K_m	$c_v(K_m)$	K_1	K_3	αK_1	αK_3	P_J%	*L*%	*F*%	T_J	Foliation	Lineation	°	′	″	°	′	″
1	*Ma*	93	16	168/19	350/69	19	14	5.8	1.6	4.2	0.43	112 S 50	202 50	22	21	1	34	0	24
2	*Ma*	152	25	178/36	355/54	4	10	5.5	3.1	2.4	−0.12	108 S 45	195 10	22	21	21	34	1	17
3	*Ma*	136	14	198/37	4/52	8	7	6.3	1.6	4.7	0.48	98 S 40	198 30	22	20	39	34	1	20
4	*Ma*	66	59	205/31	21/58	7	9	4.0	1.5	2.4	0.21	111 S 45	208 40	22	20	23	34	1	24
5	*Ma*	100	18	7/33	196/57	9	10	6.8	2.5	4.3	0.26	95 S 25	173 25	22	21	10	34	0	38
6	*Ma*	89	18	199/39	1/49	6	3	5.7	3.3	2.4	−0.16	85 S 50	193 45	22	20	49	34	1	42
7	*Ma*	75	16	193/39	19/49	6	10	7.4	3.5	3.9	0.04	115 S 50	183 50	22	20	49	34	1	57
8	*Ro*	57	5	202/20	12/70	7	4	5.5	1.9	3.5	0.29	110 S 15	208 10	22	21	15	34	3	13
9	*Ma*	50	11	211/37	359/48	9	7	5.0	2.2	2.8	0.12	93 S 40	200 32	22	20	55	34	2	26
10	*Ma*	119	26	153/18	323/70	38	23	4.1	1.5	2.6	0.27	93 S 25	na	22	20	47	34	0	11
11	*Ma*	73	9	151/4	255/69	52	38	3.9	1.0	2.9	0.46	108 S 30	183 25	22	19	58	33	59	27
12	*Ma*	46	13	195/32	34/57	7	6	2.5	1.0	1.5	0.20	114 S 35	210 35	22	20	17	33	59	45
13	*Ma*	108	22	194/36	55/47	11	16	4.6	1.8	2.9	0.23	118 S 60	215 45	22	20	20	33	59	55
14	*Kl*	23	12	218/39	13/48	8	6	2.6	1.1	1.5	0.17	103 S 65	198 40	22	18	42	33	57	28
15	*Ma*	95	14	123/24	303/65	15	19	4.2	2.4	1.8	−0.17	108 S 30	na	22	19	16	33	58	13
16	*Ma*	63	11	2/1	117/85	30	33	2.6	1.0	1.6	0.22	118 S 40	198 30	22	21	15	33	57	12
17	*Kl*	65	16	100/2	3/34	26	17	2.7	0.8	1.9	0.37	103 S 70	203 30	22	18	41	33	56	44
18	*Kl*	105	3	131/31	1/45	13	5	4.0	0.9	3.2	0.56	108 S 60	210 50	22	18	24	33	56	59
19	*Kl*	66	13	88/10	350/36	5	21	2.5	0.7	1.8	0.41	88 S 48	178 50	22	18	9	33	56	41
20	*Ro*	91	14	198/13	329/72	5	14	9.0	2.9	6.1	0.33	40 SE 50	168 35	22	23	45	34	3	25
21	*Ma*	58	29	194/32	17/57	14	6	3.2	1.5	1.7	0.08	108 S 35	173 25	22	19	18	34	1	23
22	*Ro*	69	6	194/16	47/71	6	5	5.1	1.9	3.2	0.26	98 S 25	193 25	22	19	16	34	3	6
23	*Ma*	149	36	176/27	0/71	43	35	5.3	0.9	4.3	0.64	93 S 40	163 35	22	14	38	33	58	39
24	*Ma*	126	13	138/4	44/26	32	20	3.3	1.1	2.3	0.36	128 SW 65	na	22	24	17	34	0	23
25	*Ma*	122	23	179/38	355/52	5	11	5.1	3.0	2.1	−0.18	80 S 70	na	22	24	19	34	1	23
26	*Ma*	144	17	194/25	314/47	9	32	5.2	4.0	1.1	−0.57	108 SW 30	198 30	22	29	15	33	59	9
27	*Ro*	213	18	206/21	10/76	42	34	3.2	2.2	0.9	−0.41	48 SE 30	212 12	22	33	11	34	0	35
28	*Ma*	118	19	194/63	8/27	9	10	9.3	4.2	5.0	0.07	100 S 70	10 30	22	30	55	33	59	47
29	*Ma*	148	20	185/57	21/32	7	17	9.7	4.5	5.2	0.05	100 S 70	20 30	22	30	55	33	59	47
30	*Ma*	96	11	206/34	16/55	9	18	7.7	3.3	4.4	0.12	110 S 45	15 55	22	30	55	33	59	47
31	*Ma*	59	21	213/14	345/62	36	31	2.8	0.7	2.2	0.53	98 S 30	210 30	22	18	44	33	57	53
32	*Ma*	25	20	126/45	317/47	38	12	1.1	0.3	0.8	0.47	80 S 80	107 0	22	18	46	33	57	34
33	*Kl*	27	3	223/24	0/59	7	4	4.3	1.0	3.3	0.54	92 S 30	202 30	22	18	45	33	57	19
34	*Ma*	99	7	168/28	2/61	6	8	4.3	1.9	2.3	0.08	100 S 30	206 20	22	20	41	33	58	14
35	*Ma*	61	18	212/30	337/45	4	3	4.4	2.0	2.4	0.07	98 S 31	237 22	22	20	55	34	2	34
36	*Ma*	46	8	206/35	348/48	7	3	4.7	1.4	3.4	0.42	87 SE 55	222 40	22	21	3	34	2	33
37	*Ma*	44	12	204/15	322/60	6	4	4.0	1.2	2.8	0.41	72 SE 30	227 10	22	21	15	34	2	35
38	*Ma*	77	18	194/36	5/53	4	5	7.8	3.6	4.1	0.05	122 S 36	222 32	22	20	51	34	2	15
39	*Ro*	121	15	197/15	65/68	9	5	3.6	1.6	2.0	0.08	180 W 20	227 10	22	21	29	34	3	15
40	*Ro*	56	9	210/22	33/69	23	4	3.1	0.8	2.3	0.47	127 S 15	200 15	22	21	26	34	2	48

41	*Ma*	110	30	182/33	25/55	5	36	2.3	1.4	0.9	−0.21	110 S 35	na	22	21	12	34	0	49
42	*Mo*	566	9	207/34	349/49	6	7	25.7	9.9	15.8	0.18	90 S 40	na	22	30	55	33	59	47

[a] Rock types and mineral assemblages: *Kl* = Kleinfontein leucogranite (Kfs–Pl–Qtz–Bt–Grt–Tur–Fl), *Ma* = Maalgaten granite (Kfs–Pl–Qtz–Bt–Ilm ± Grt ± Tur ± Czo ± Crd), *Ro* = Rooiklip granite gneiss (Kfs–Pl–Qtz–Bt–Ilm ± Grt ± Ms), *Mk* = Modderkloof granodiorite (Kfs–Pl–Qtz–Bt–Mt). Symbols after Kretz (1983). K_m = mean magnetic susceptibility of the station in μSI; $c_v(K_m)$ = within-station variability of K_m; K_1 = trend and plunge of the magnetic lineation (in degrees); K_3 = trend and plunge of the pole of the magnetic foliation; αK_1 and αK_3 = within-station mean angular variabilities (in degrees) of the specimen; P_J% = total anisotropy of the magnetic susceptibility; L% = linear magnetic anisotropy; F% = planar magnetic anisotropy; T_J = Jelinek's parameter; na = not available.

Czo–Ep assemblages are common in the Soetkraal Formation. The Victoria Bay Formation contains Cal–Di–Bt–Kfs–Grs–Ves–Wo–Ttn. Garnet and fibrolite hornfels are common near the contact with the granites.

3. Structures

New field observations have been collected to establish more precisely the kinematic setting of the Saldanian basement and its relationship with contact and regional metamorphisms. The contact between the Kaaimans inlier and the Cape Fold Belt is generally characterised by a high strain zone a few tens of metres in width with numerous quartz-filled tension gashes, mylonites and asymmetric folded quartz veins indicating a consistent top-to-the-north sense of shear. Away from this zone the Cape orogeny overprint vanishes over short distances.

3.1. Country rocks

The metasedimentary formations of the Kaaimans Group trend in an east–west direction (Fig. 2) with dips towards the south, and generally exhibit penetrative planar and linear fabrics (Fig. 3). Bedding (S_0) is transposed into a bedding-parallel metamorphic banding (S_{0-1}). In the easternmost and westernmost parts of the Kaaimans inlier, at distance from the plutons, the Homtini Formation dominantly consists of shales. Together with preserved sedimentary structures, such as channels filled with feldspar arenites showing graded bedding, this constrains regional metamorphism prior to granite intrusion to a very low grade. Cross-bedding and graded bedding in quartzites and grits, preserved in a few low-strain zones, and away from the intrusives, can be used as polarity criteria. These are right-way-up except in overturned fold limbs. A crenulation cleavage is observed in the Homtini Formation only towards the plutons. Closer to the plutons, an east–west-striking foliation (S_1) overprints the banding with dips decreasing gradually from 70°S in the north to 20°S in the south. The Saasveld, Skaapkops and Victoria Bay formations display boudinaged layers of quartzites and pelites (Fig. 4a). Mineral stretching lineations (L_1) are ubiquitous and marked by the long axes of andalusite (Fig. 4c) and the elongated aggregates of muscovite or biotite crystals. L_1 plunges moderately to the SSW (Fig. 3). Asymmetric minor drag-folds are commonly observed in the schists. Tight recumbent folds, with fold axes around 305° 20°, occur locally at the western and eastern ends of the George pluton. Sheath folds, with axes parallel to L_1 occur, to the south of the George pluton, for example near station #20 (Fig. 2), suggesting a locally high strain

zone. Fold amplitudes vary from a few centimetres in the Soetkraal schists to a few hundreds of metres in the Saasveld schists. The fold axial planes are usually parallel to a steep crenulation cleavage that cross-cut S_{0-1} and dips to the south. This cleavage occurs in most units that display a schist lithology throughout the Kaaimans inlier. Finally, shear-sense indicators, such as asymmetric boudins (Fig. 4a), *C–S* structures (Fig. 4b) and drag-folds, consistently give a top-to-the-north sense of shear.

The top-to-the-north sense of shear is also supported by various structural features at different scales. Several shear zones, parallel to the main foliation, anastomose into *C–S* structures a few metres wide forming a larger 50-m-wide shear zone in the Sandkraal quartzites to the east of the George pluton. The geometry of these large-scale *C–S* structures is identical to that of the smaller ones (see Fig. 4b). The conglomerates of the Skaapkops Formation contain clasts of up to 5 mm in diameter with asymmetric wings and *C–S* structures.

Two populations of andalusite porphyroblasts occur (Fig. 4c) in the contact aureole, only in pelitic beds. They occur less than 300 m from each pluton of the Kaaimans inlier and are absent elsewhere. The first population (A1, Fig. 4c inset) is restricted to the aureole. The corresponding porphyroblasts are rimmed by sigmoidal biotite aggregates, and display pressure shadows. These andalusite porphyroblasts are thoroughly sericitised, flattened parallel to S_1 and elongated parallel to L_1. They record a top-to-the-north sense of rotation. This is consistent with mineral growth during granite intrusion. Andalusites of the second population are euhedral and non sericitised crystals (A2, Fig. 4c inset). These andalusites, less well oriented than those of the first population, grew slightly oblique to S_1.

3.2. Plutonic rocks

The George pluton outcrops concordantly between formations of contrasting lithologies in the Kaaimans inlier: the Saasveld Formation at its base, and either the Sandkraal or Skaapkops Formation at the top. The northern margin of the pluton is characterised by numerous boudinaged pegmatite veins, microgranite sills and albitite lenses in the country rock. These felsic rocks are abundant close to the pluton contact and are probably connected to the Kleinfontein leucogranite.

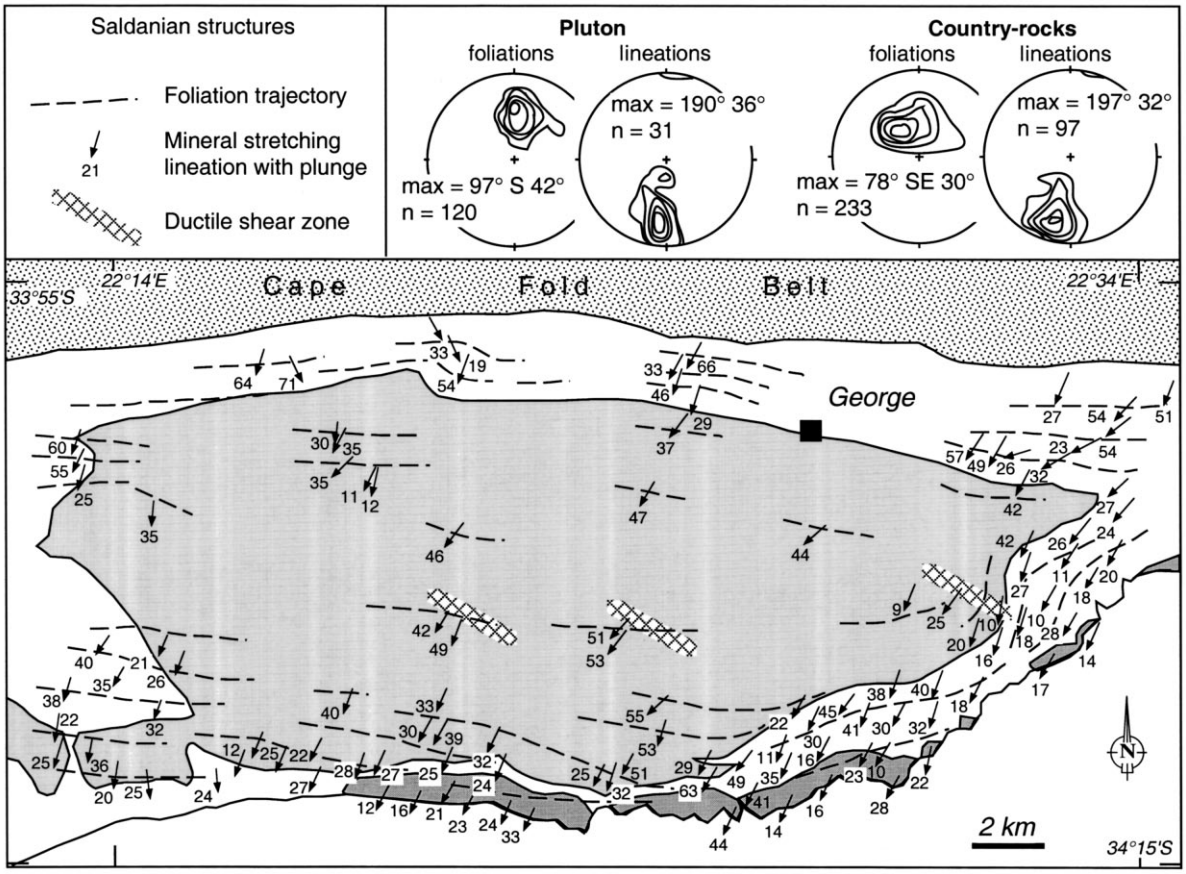

Fig. 3. Regional structures of the George pluton and the country rocks in the Kaaimans inlier. The inset shows stereonets of the poles to foliation and lineations. Lower hemisphere projection, equal area, 1% contour area, 1–2–3–4–5% contour lines.

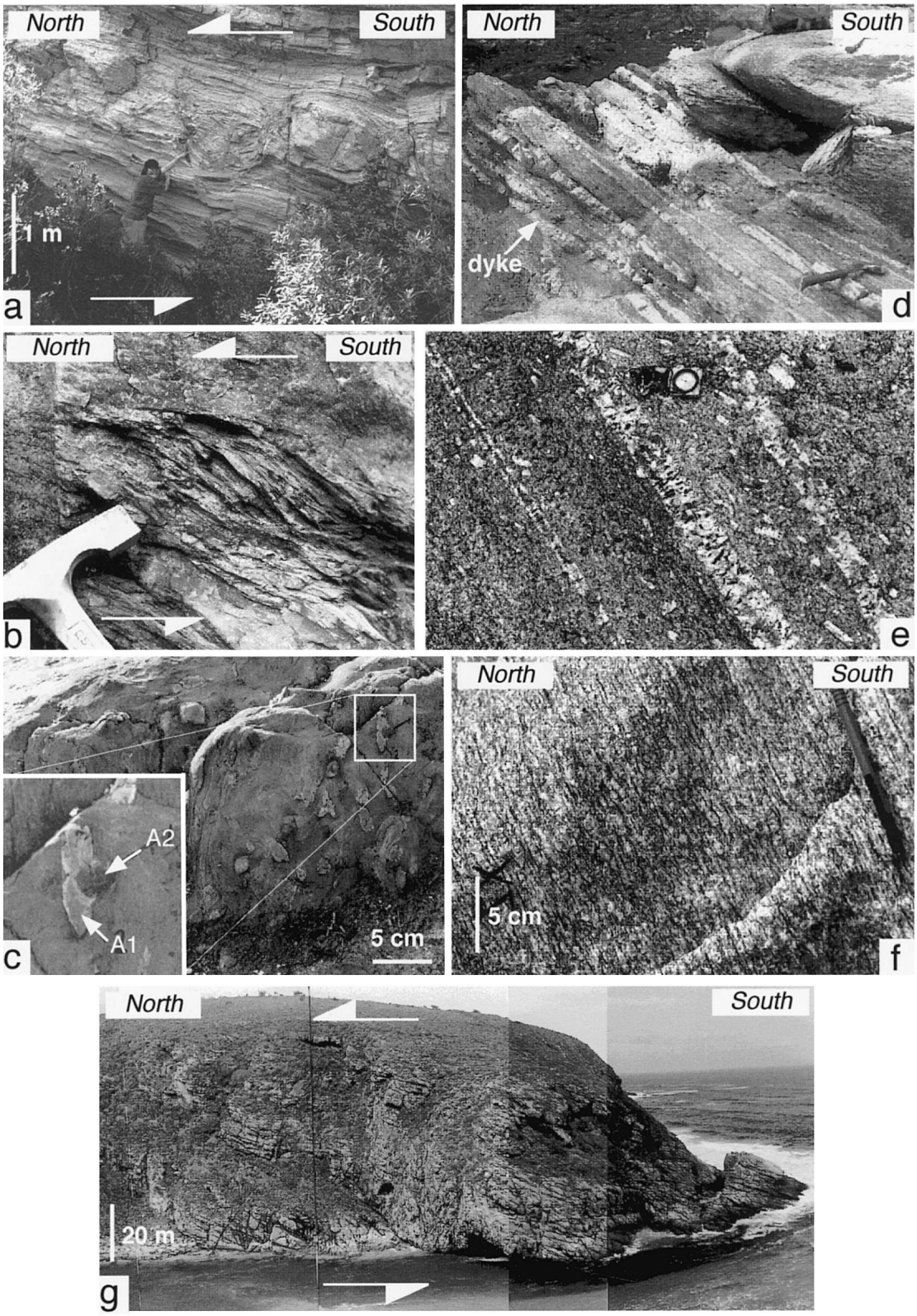

Fig. 4. Field photographs of rock structures in the Kaaimans inlier. Localisations are shown on Fig. 2. (a) Asymmetric boudins in the Soetkraal Formation indicating a top-to-the-north sense of shear. (b) Top-to-the-north *C–S* structures in the Sandkraal quartzites. (c) Two populations of andalusite porphyroblasts in the contact aureole. The first population (noted A1) grew during granite intrusion: andalusites are flattened parallel to foliation and elongated parallel to lineation. In the second one (noted A2), the andalusites are barely oriented. (d) Pegmatitic dykes parallel to foliation in the Kleinfontein leucogranite. (e) Comb structures in pegmatitic dykes with tourmaline crystals perpendicular to the walls, in the Maalgaten granite. (f) Penetrative gneissic structure of the Rooiklip granite. (g) Panoramic view of the Rooiklip granite with a south-dipping foliation.

The southern margin, well exposed, displays a conformable contact (dips between 20° and 50°) with the country rocks. Mylonitic deformation occurs everywhere along the southern margin of the pluton. Undeformed pegmatitic dykes, 10 cm in width, and dipping gently to the south, cut through the George pluton (Fig. 4d). Tourmaline crystals in these dykes grew perpendicular to the dyke walls (Fig. 4e). The whole pluton displays a penetrative gneissic structure, characterised by K-feldspar augen surrounded by biotite crystals and forming *C–S* structures (Fig. 4f). The matrix crystals are parallel to the *S*-planes and define the pervasive foliation with, on average, dips 15°S against 30°S for the *C*-planes. The *C*-planes, although less penetrative, are often more prominent than the *S*-planes. Ellipsoidal mafic enclaves and xenoliths of restitic country rock are parallel to the foliation with their long axes parallel to the stretching lineation. This lineation is pervasively underlined by the alignment of the K-feldspar megacrysts. Three ductile normal shear zones, a few metres to a few tens of metres in width, cut through the George pluton (Fig. 2: stations #24 and #28 and Fig. 3). They strike N120° and dip around 70°S with down-dip lineations and normal shear sense. This sense of shear is exceptional in the region. In turn, these shear zones are crosscut by non-foliated pegmatite dykes of a few tens of centimetres in width.

The Rooiklip granite also exhibits a penetrative gneissic structure with a south-dipping foliation (Fig. 4g), open drag-folds and asymmetric kink-folds indicating a top-to-the-north sense of shear. By contrast with the Maalgaten granite of the George pluton, the occasional xenoliths of Soetkraal schists (1×0.4 m^2) are angular. A few centimetre-thick shear bands are parallel to the *C*-planes and are visible over at least a few metres.

Shear sense indicators such as *C–S* structures in the George and the Rooiklip plutons and their country rocks have a top-to-the-north sense with a slight sinistral component. Some of the above-mentioned structures, such as the crenulation cleavage, have been interpreted previously as resulting from a Cape orogeny overprint (e.g. Gresse, 1983). This view is not supported by our field observations presented above and needs to be confronted with detailed microstructural observations.

4. Microstructures

Microstructural observations are based on representative and oriented thin sections. Thirty-five thin sections were cut from the country rocks in the XZ plane, and 42 from the granites, out of the AMS cores (see Section 5). Lattice Preferred Orientations (LPO) have been checked using a sensitive tint plate. Microstructural terminology follows that of Passchier and Trouw (1996).

The Cape Fold Belt quartzites, along the contact with the Kaaimans inlier, are characterised by cataclastic and mylonitic microstructures, with quartz ribbons and undulose extinction in quartz grains.

The Kaaimans country rocks display sedimentary structures. These are prominent at distance from the plutons (> 5 km), in the Homtini Formation, in spite of discrete cleavage. They include laminations and compaction microstructures in shales, with grain size of 50 μm in quartz–sericite schists, and graded bedding in arenites with quartz pebbles displaying undulose extinctions and sharp prism–subgrain boundaries. Evidence of pressure solution along the cleavage and foliation plane is provided by well-developed crenulation cleavage in the Soetkraal schists, and truncated fold hinges within quartz layers in the Silver River phyllites. Close to the plutons, metasediments exhibit contact metamorphism microstructures accompanied by a pervasive static recrystallisation, especially in the Saasveld, Sandkraal and Skaapkops formations. Andalusite porphyroblast size increases towards the contact with the granites in the Saasveld schists. In all the formations, quartz grain aggregates form lenses or ribbons, with polygonal microstructures. The quartz aggregates display pronounced LPOs acquired before static recrystallisation. Feldspars show pinning and bulging microstructures suggesting grain-boundary migration. Shear sense indicators such as rotated porphyroblasts (Fig. 5a), mica fish (Fig. 5b) and *C–S* microstructures (Fig. 5c) consistently indicate a top-to-the-north sense of shear.

The George pluton rocks display various microstructures indicating that a more or less pronounced recrystallisation occurred throughout the pluton. The original quartz grains (up to a few millimetres in length) tend to occur in lens-shaped aggregates with length/width ratios 3 and strong LPOs. These grains are almost free of undulose extinction and display polygonal microfabrics even in shear zones (e.g. Kraaibos quarry, stations #28–30; Fig. 2). Quartz seldom forms smaller grains ranging from 100 to 400 μm, displaying smaller grain sizes, dynamic recrystallisation microstructures, parallel deformation bands, and grain boundary migration microstructures (Fig. 5d). In places, recrystallised quartz grains may be even smaller, down to 10 μm in length. All these features contrast with the grain size displayed by alkali feldspar and plagioclase grains (200 μm to a few cm in length). In numerous localities, within the George pluton, alkali feldspar and plagioclase megacrysts show fractures filled with fine quartz and feldspar grains (Fig. 5e). Aggregates of similar fine-grained quartz and feldspar formed in recrystallisation wings and at the

periphery of the alkali feldspar megacrysts. Biotites are often bent (Fig. 5f) or kinked and cast around alkali feldspars, thus forming augen microstructures. In a few stations near the centre of the pluton (#2, #6 and #41), biotite grains are significantly smaller than in the rest of the pluton and form clusters suggesting their recrystallisation. Shear sense indicators such as *C–S* microstructures and antithetic microfaults in megacrysts are very common and consistently indicate a top-to-the-north sense of shear.

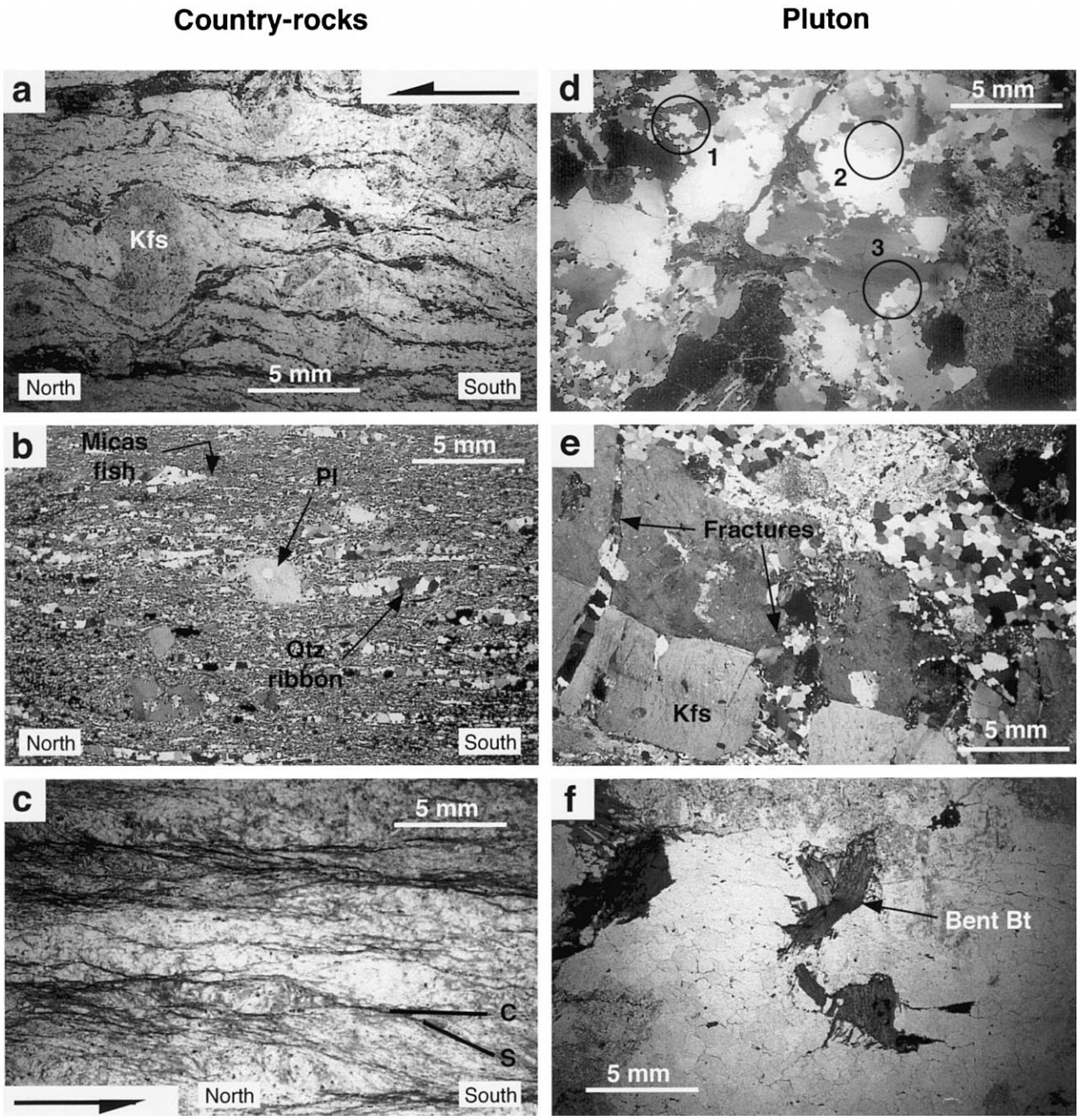

Fig. 5. Microstructures of the Kaaimans inlier country rocks in *XZ* sections (a, b and c), and of the George pluton (d, e and f). (a) Skaapkops quartzo-feldspathic schists: rotated porphyroblasts of feldspar in the indicating a top-to-the-north sense of shear. (b) Sandkraal quartzites: micas fish, and quartz pervasive recrystallisation into ribbons and mosaics of equant grains. (c) Soetkraal schists: *C–S* microstructures (top-to-the-north sense of shear). (d) Maalgaten granite: dynamic recrystallisation, prism-deformation bands and grain boundary migration microstructures. (e) Maalgaten granite: submagmatic fractures in feldspars filled with quartz and feldspar. (f) Maalgaten granite: bent biotites. Abbreviations: Kfs = alkali feldspar, Qtz = quartz, Pl = plagioclase, Bt = biotite.

5. Magnetic fabrics

5.1. Principles and method

The investigation of the low-field magnetic anisotropy is now well established in the study of granitic rocks (see references in Bouchez, 1997; Borradaile and Henry, 1997). The basic theory expresses that a rock sample modifies the intensity of the applied low magnetic field in which it is immersed. The ratio between the induced magnetisation and the inducing magnetic fields is named the magnetic susceptibility and noted K. This magnetisation disappears when the field is relaxed. Spatial variations of magnetic susceptibility are represented by an ellipsoid with K_1, K_2 and K_3 as principal axes ($K_1 \geq K_2 \geq K_3$). K_1 corresponds to the magnetic lineation, and K_3 is the pole to the magnetic foliation. The mean magnetic susceptibility K_m is the arithmetic mean of the principal axes [$K_m = 1/3 (K_1 + K_2 + K_3)$]. The variation coefficient of the magnetic susceptibility is $c_v(K_m)$ [$c_v(K_m) = 100 \times \sigma(K_m)/K_m$, in %] where $\sigma(K_m)$ is the standard deviation of K_m. The total anisotropy is given by $P_{Jelinek}$% [$P_J\% = 100 \times [(\exp[2 \Sigma (\ln K_i/K)^2]^{1/2})-1]]$ (i = 1–3). The linear and planar anisotropy components are, respectively, given by L% [$L\% = 100 \times [(K_1/K_2)-1]]$ and F%

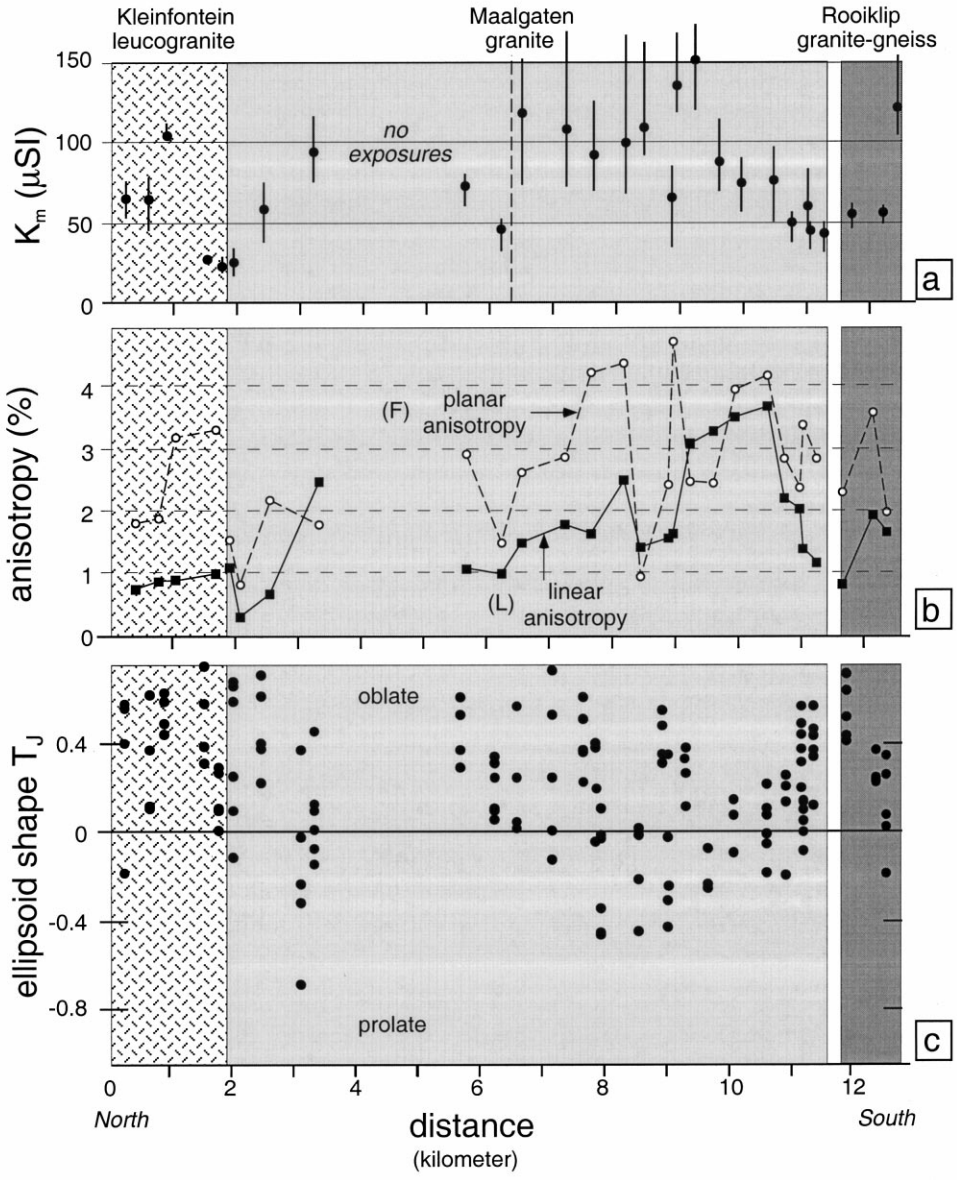

Fig. 6. Profiles XX' (see location in Fig. 2) of magnetic anisotropies across the George pluton. (a) Susceptibility magnitudes K_m (in μSI). Note the high K_m in the south central part with values broadly decreasing towards the margins of the pluton. (b) Planar anisotropy F% and linear anisotropy L%. Note the increase of L% towards the south and the drops of L% near the southern lithological boundaries. (c) T_J shape parameter (Jelinek, 1978): $T_J > 0$ for oblate ellipsoids; $T_J < 0$ for prolate ellipsoids. Note that most samples have oblate AMS ellipsoids.

$[F\% = 100 \times [(K_2/K_3)-1]]$. The total anisotropy, together with the linear and planar anisotropies have been corrected for the influence of the diamagnetic quartzo-feldspathic matrix (Rochette, 1987). The shape of the ellipsoid is represented by the parameter T_{Jelinek} $[T_J = 2 \times (\ln K_2 - \ln K_3)/(\ln K_1 - \ln K_3) - 1]$ (Jelinek, 1978).

Specimens were obtained from 42 stations within the George pluton (see localities in Fig. 2 and values in Table 1). Most stations are in the Maalgaten River gorge (Fig. 1), along a NNW–SSE section, at an average spacing of 500 m. Each station was positioned with a GPS portable unit with an accuracy of ±25 m in latitude and longitude in the WGS84 system. Two oriented cores per station were collected in the field with a portable drill at each station, at a distance of 1–2 m from one another. The weathered part of the samples, usually limited to the top 2 mm, has been removed. Cores were long enough to yield at least two samples, giving at least four samples per station. A

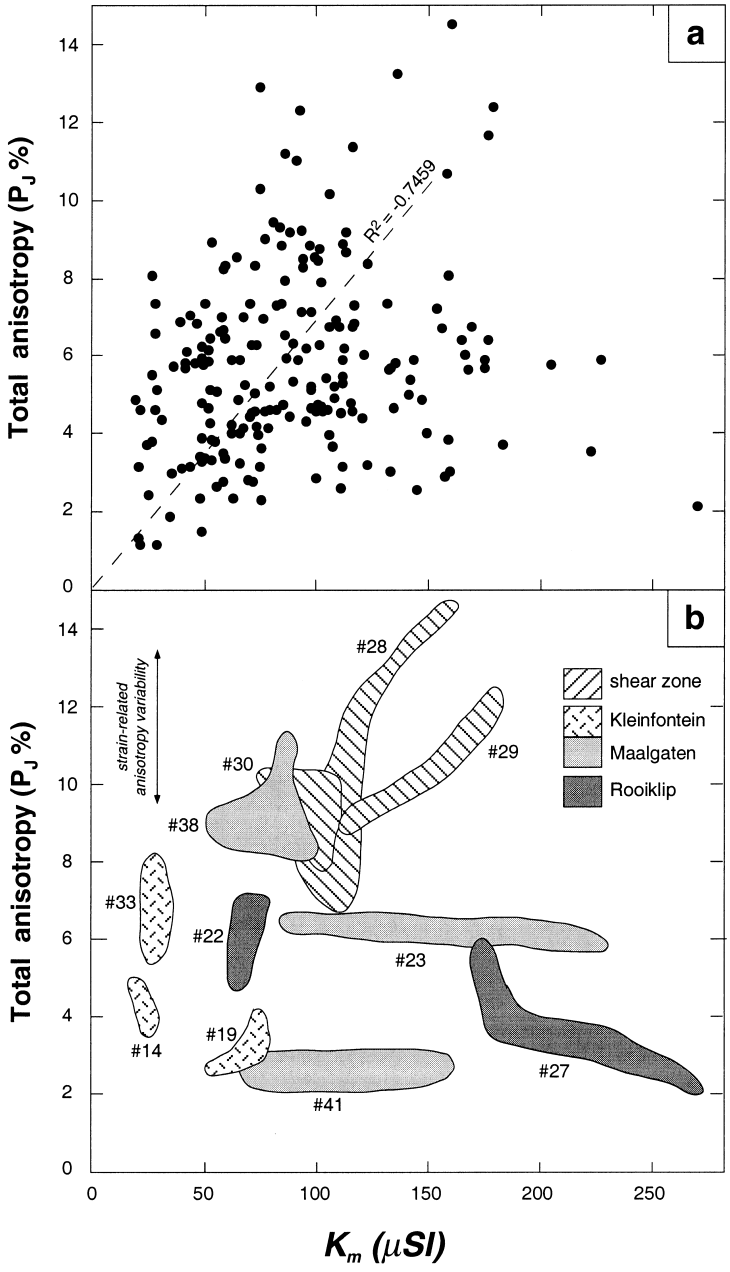

Fig. 7. Magnetic susceptibility anisotropy P_J (in %) vs. magnetic susceptibility K_m (in μSI). (a) Positive correlation at the scale of the pluton. Dash line represents the regression line. (b) The positive correlation P_J–K_m is not generally observed within a sampling station, except in samples from the shear zone. Note that: within-station ΔP_J is < 2% except in the shear zone; within-station ΔK_m is larger in the coarse grained rock types.

total of 206 samples have been analysed. The cores, of a diameter of 25 mm, were cut at a standard length of 22 mm to conform with the length/diameter ratio of 0.85 recommended by Noltimier (1971) for magnetic measurements. The measurements of the magnetic susceptibility and its anisotropy were carried out at low alternating inductive magnetic field ($\pm 4 \times 10^{-4}$ T, 920 Hz) on a Kappabridge KLY-2 susceptometer (Agico, Brno). This highly sensitive apparatus provides reliable and reproducible values over a wide range of susceptibilities (0.05 μSI to 0.5 SI) and low anisotropies (down to 0.2%). Angular dispersion of the magnetic ellipsoid axes due to measurement procedure are usually less than 5°. Finally, one thin section was made for each station from one of the cores to correlate the AMS parameters with microstructures.

5.2. Mean magnetic susceptibility

The mean magnetic susceptibility K_m of each station displays widely overlapping ranges within the petrographic units (Table 1). At the scale of each core sample, K_m varies from 19 to 108 μSI in the Kleinfontein leucogranite ($K_m \pm 1\sigma = 56 \pm 32$ μSI; $n = 21$ samples), 20–227 μSI in the Maalgaten granite ($K_m \pm 1\sigma = 92 \pm 42$ μSI; $n = 151$), 49–270 μSI in the Rooiklip granite gneiss ($K_m \pm 1\sigma = 99 \pm 55$ μSI; $n = 27$) and 473–614 μSI in the Modderkloof granodiorite ($K_m \pm 1\sigma = 566 \pm 55$ μSI; $n = 5$). The Kleinfontein unit typically displays the lowest K_m while the Modderkloof unit, although characterised by only one station, displays the highest K_m. The within-station variation coefficient for K_m, larger in the coarser grained rocks, are 9% in the Kleinfontein and Modderkloof units, 11% in the Rooiklip unit and 19% in the Maalgaten unit. However, on the profile of K_m values across the pluton (Fig. 6a), the Maalgaten granite displays lower K_m towards its margins. Furthermore, the northern half of the pluton shows lower K_m than the southern half.

5.3. AMS scalar data

The magnetic anisotropy data for each station are listed in Table 1. The anisotropy percentages (P_J%) range from 1 to 14% (average ≈ 5%) with 80% of samples ranging from 2 to 6%. In the Modderkloof granodiorite, P_J% ranges from 17 to 35% (average = 26%). The linear anisotropy (L%) ranges from 0.2 to 7.1% (average ≈ 2%) while the planar anisotropy (F%) ranges from 0.2 to 7.2% (average ≈ 3%). The within-station variation of both the linear and the planar anisotropies is less than 2% except in a shear zone (stations #28–30) where it reaches 5%.

In the profile across the George pluton (Fig. 6b), F% is found to be broadly correlated with L%, with $F\% > L\%$. The anisotropy magnitude, measured either by P_J%, F% or L%, is higher in the south central part of the George pluton than in the north where decreasing values towards margins are observed. In stations where $L\% > F\%$, biotite grains are observed to be recrystallised (stations #2, #6 and #41) or the rock to be weathered (#15). Stations from the mylonitic southern rim of the George pluton have moderate anisotropy magnitudes 4%, and cannot be distinguished from the rest of the pluton. The parameter T_J, plotted along the same profile (Fig. 6c), shows that the magnetic ellipsoids are oblate in shapes except in the south-central part of the pluton where some prolate ellipsoids occur.

At the scale of the pluton, P_J% and K_m display a coarse positive correlation marked by a dash line on Fig. 7(a). However, at the scale of the stations, P_J% and K_m exhibit independent behaviours. P_J%–K_m plots between samples from a few representative stations (Fig. 7b) show that: (i) the within-station variation of P_J% is less than 2% except in the shear zone; (ii) the within-station variation of K_m is larger in the coarse grained and porphyritic granites (Maalgaten unit) than in the fine grained ones (Kleinfontein unit); and (iii) the largest variation in P_J% comes from the shear zone (stations #28–30) where the highest anisotropy $P_J \approx 14\%$ is recorded.

5.4. Directional data

The principal axes K_1 and K_3 of the magnetic ellipsoid are represented together with field structural data in the stereonets of Fig. 8. The directional data show a limited within-station variability represented by the average departure angle αK_i ($i = 1$ and 3, see Table 1) usually less than 20°. Data consistency throughout the George pluton is noticeable, particularly along the Maalgaten River section (Fig. 9): the mean foliation is at 100° S 35°, and the mean lineation is at 200°, 33°. These directional data are consistent with field structural data (Table 1) except in a few tourmaline-bearing samples of the Kleinfontein leucogranite (Fig. 8: specimens labelled as 'Tur'). The dip angle of magnetic foliations is usually less than that of the field foliation, measured on the C-planes, as illustrated in Fig. 10.

6. Discussion

6.1. Saldanian basement/Cape Fold Belt relationships

The Cape Fold Belt is a foreland thrust-fold orogen formed between 280 and 220 Ma (de Wit and Ransome, 1992). The Saldanian Belt, the basement of the Cape Fold Belt, resulted from regional thrusting between 600 and 520 Ma (Thomas et al., 1993). The

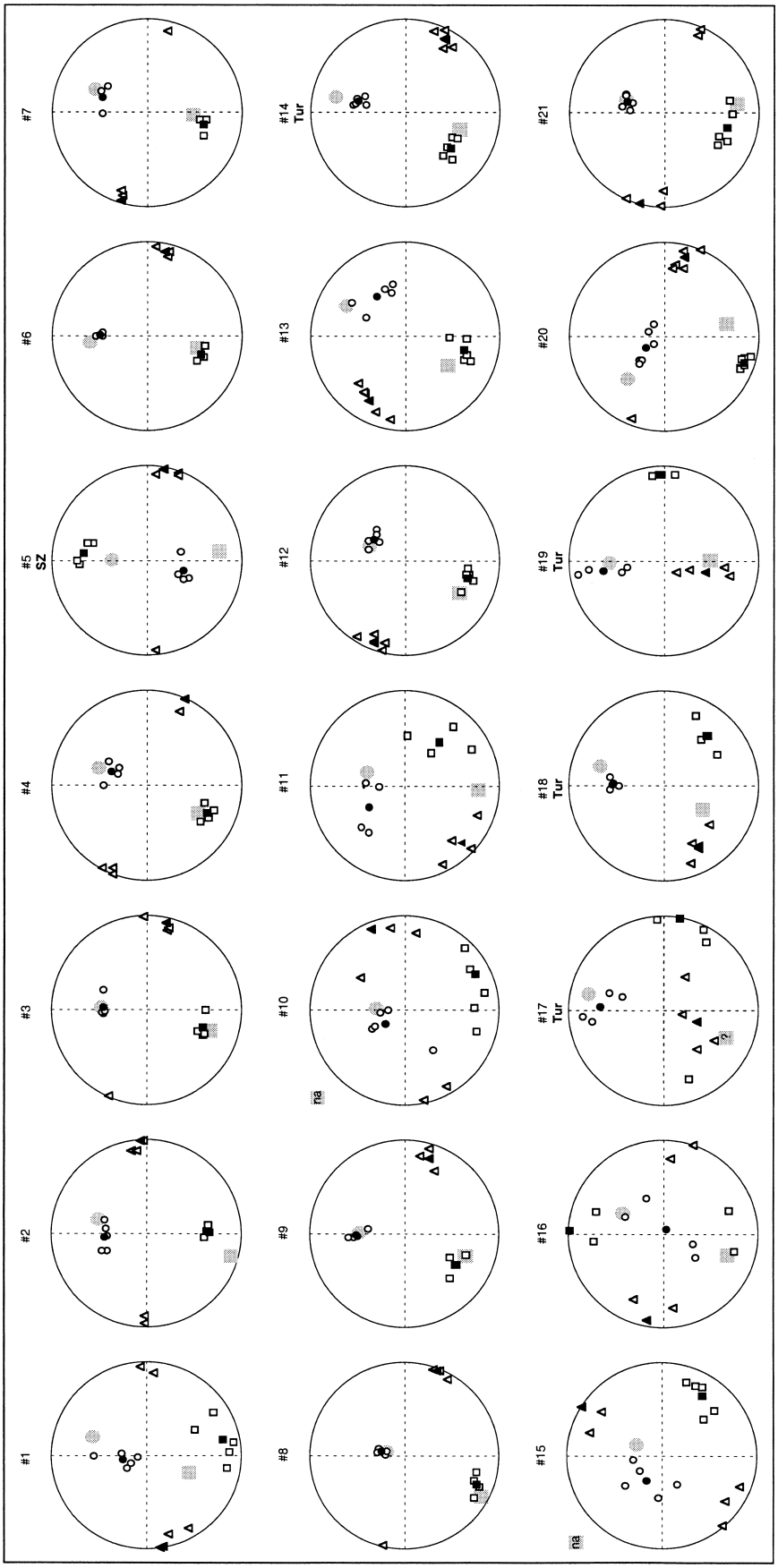

Fig. 8. Orientations of magnetic fabrics and field structures for the 42 stations of the George pluton. Wulff stereonets, lower hemisphere projection. Small symbols = magnetic fabrics (squares = K_1; triangles = K_2; circles = K_3), open symbols = core samples, filled symbols = mean of at least four samples per station. Grey symbols = field structures (squares = mineral lineation; circles = poles to the foliation). Tur = Tourmaline; na = not available.

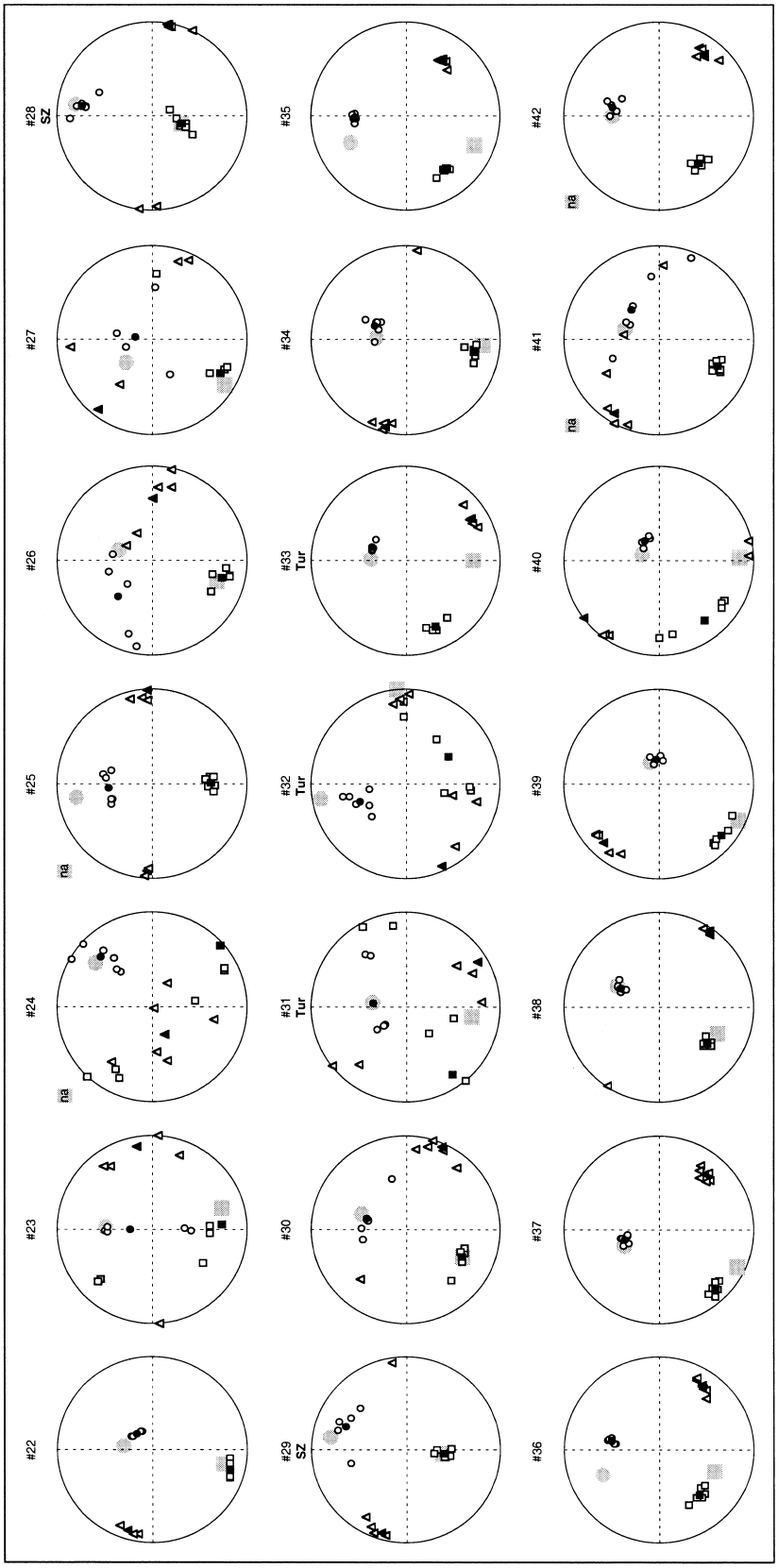

Fig. 8 (*continued*)

metamorphic peak conditions of the Cape orogeny, a few kilometres north of George town, have been estimated to 2.5 kbar and 350°C by Hälbich and Cornell (1983). The lowest pre-intrusion metamorphic conditions in the Kaaimans inlier are constrained by the stability of primary illite–smectite in the Homtini Formation to < 300°C (Frey and Robinson, 1999). Therefore, the thermal conditions of the Saldanian and Cape orogenies largely overlap. This thermal similarity has led Gresse et al. (1992) to conclude that the Kaaimans inlier underwent a substantial Cape overprint. However, this does not take into account the >200 My gap between each tectonic event. The basement–cover relationship interpreted by Söhnge and Hälbich (1983) as a thick-skin tectonics but no Cape microstructural overprint is observed in the Kaaimans inlier. In the highest unit of the Kaaimans stratigraphy, i.e. the Homtini Formation (Gresse, 1983), deformation was moderate as indicated by the well-preserved sedimentary structures. By contrast, the Cape rocks close to the Kaaimans inlier display intense folding and shearing together with pervasive recrystallisation features. These observations together with the high strain zone commonly observed all along the contact between

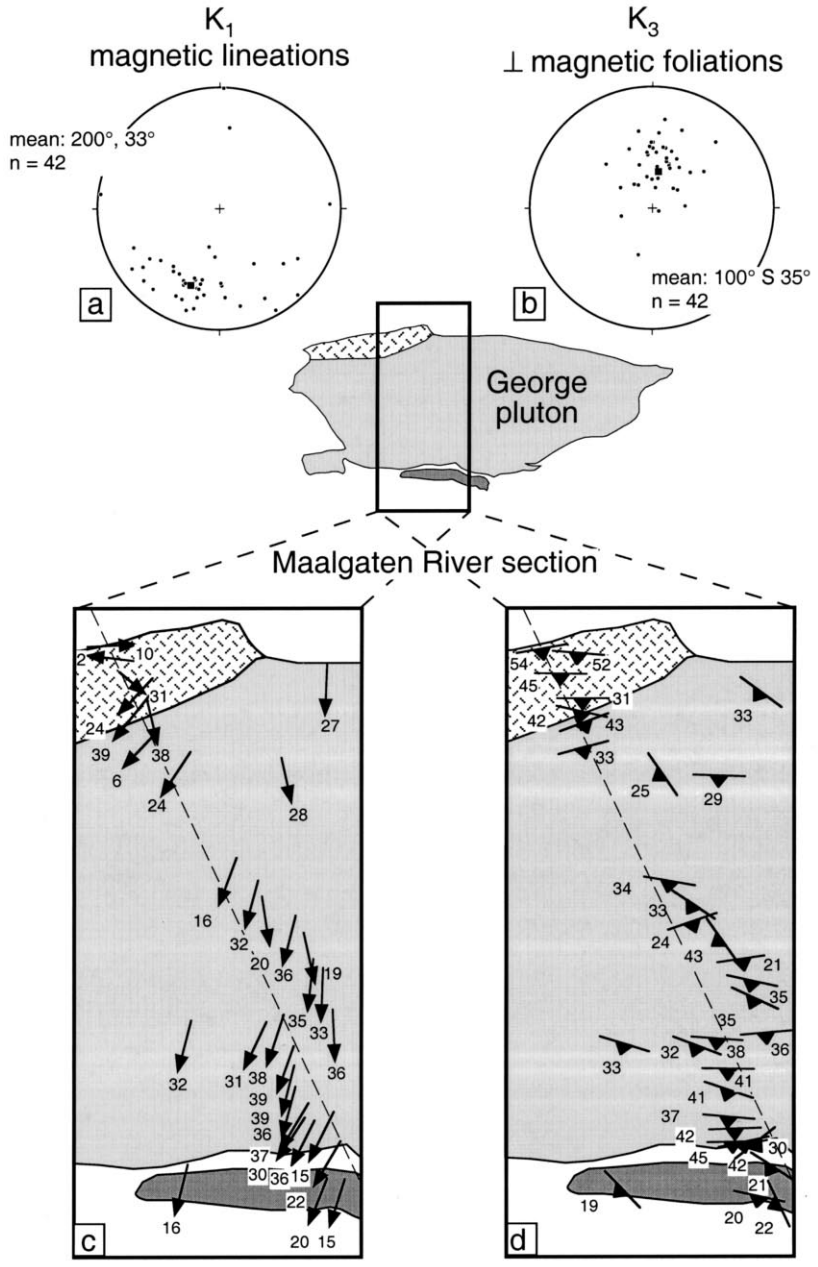

Fig. 9. Maps of magnetic fabrics along the Maalgaten River section (see location in Fig. 2) in the George granites. (a and c) K_1-lineations. (b and d) K_3-foliations.

the Kaaimans inlier and the Cape Fold Belt, suggest a late mechanical decoupling between the basement and its cover.

6.2. Saldanian kinematic setting

Even though Krynauw (1983) had shown that regional deformation was coeval with granite emplacement, the Saldanian tectonic framework has not been precisely established. Planar and linear structures in the Kaaimans metasediments around the plutons are penetrative and very consistent. Foliations strike in an east–west direction with moderate southerly dips while lineations trend SSW with moderate plunges (Fig. 3 inset). Kinematic criteria such as *C*–*S* structures, oblique clasts on the foliation, asymmetric porphyroblast wings and pressure shadows, asymmetric drag-folds and boudins, consistently indicate top-to-the-north sense of shear (Fig. 4). The George pluton dips to the south in conformable contact with the country rock foliation. Planar and linear mineral fabrics are strong, fairly penetrative, very consistent and similar in orientation to those in the country rock (Fig. 3 inset). Ellipsoidal mafic enclaves display ductile deformation features and are elongate parallel to the mineral stretching lineation together with the *C*-axes of Kfs megacrysts. These features are characteristic of magmatic to near-solidus condition of deformation and this is incompatible with the Cape tectonic overprint hypothesis. Kinematic criteria such as ubiquitous *C*–*S* structures and domino-structures in Kfs megacrysts consistently indicate top-to-the-north sense of shear (Fig. 10). The three steep south-dipping normal ductile shear zones observed in the George pluton (Fig. 3) may result from strain partition domains forming a conjugate system with the moderately dipping reverse *C*–*S* structures. Similar *C*–*S* structures are observed in the Rooiklip granite where asymmetric drag-folds and kink-folds again indicate a consistent top-to-the-north kinematics (Fig. 4f and g). The above observations support the theory that granite emplacement occurred during thrust deformation of the country rock. The *C*–*S* structures and shear zones are cut by non-foliated pegmatite dykes. Since no plutonism is known to occur during the Cape orogeny, these pegmatite dykes are probably Saldanian in age, and probably late-magmatic differentiates. Therefore, a consistent Saldanian top-to-the-north thrust kinematics occurred during granite intrusion along with no substantial Cape tectonic overprint.

The distribution of metamorphic grades in the Kaaimans inlier has been interpreted as an inverted regional metamorphic sequence with higher grade rocks towards the top, i.e. the south (Frimmel and van Achterbergh, 1995). An alternative way of explaining this distribution would be if the whole Kaaimans inlier had been overturned. This can be ruled out because sedimentary way-up criteria in metaconglomerates and sandstones between the George pluton and the Rooiklip sill indicate a normal polarity. We suggest that the observed distribution of metamorphic grades results from the combination of both regional and contact

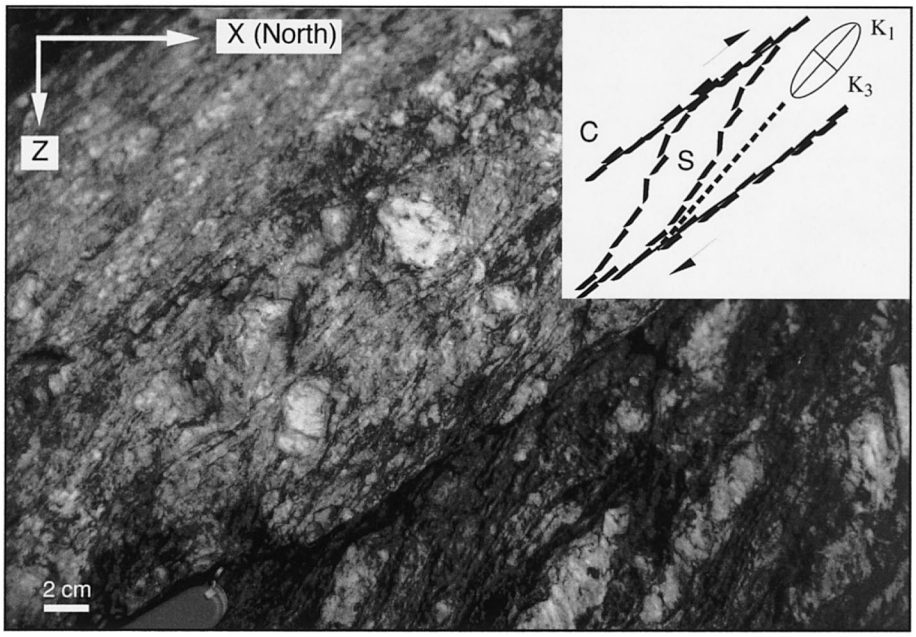

Fig. 10. Macrophotograph of typical gneissified George pluton: *C*–*S* structures and magnetic significance. The biotite-controlled magnetic fabric (ellipsoid and dashed line in the inset) lies in between the *C*- and *S*-planes. Consequently, the obliquity between field foliation (*C*-planes) and magnetic foliation can be used as a shear-sense criteria, conformably to '*S*' sigmoid at tips of Kfs megacrysts.

metamorphism and that the inverted sequence has not been unambiguously established.

6.3. Contact metamorphism

The two populations of andalusite porphyroblasts are restricted to aureoles around the intrusives and therefore do not result from regional metamorphism prior to the intrusions. These two populations display distinct relationships with respect to the timing of deformation. The first population of andalusites (A1 on Fig. 4c), parallel to the regional foliation S_1 and elongated parallel to the stretching lineation, is synkinematic. The second population forms stocky porphyroblasts (A2 on Fig. 4c), displaying much less preferred orientation, and this suggests a late to post-kinematic growth with respect to pluton emplacement.

The existence of two successive populations of andalusites inevitably requires an intrusion-related metamorphic history with two thermal events. Such a thermal history could be explained by a multiple injection and reheating of the country rocks (e.g. Nyman et al., 1995) or by a single injection with succession of heat transfer mechanisms. Multiple injections may occur at the scale of one pluton, e.g. the George pluton made up of distinct petrographic types (Kleinfontein, Maalgaten and Modderkloof). At the scale of the whole Kaaimans inlier, the Great Brak River, George and Woodville plutons may have been emplaced successively ($\approx$535 Ma) also resulting in a complex thermal history. This model, however, does not easily explain either the contrasted relationships to the timing of deformation (i.e. syn- vs. post-kinematic) nor the sericitised/not sericitised character of the two andalusite populations. In a single injection hypothesis, the interplay between different mechanisms may result in two apparent thermal peaks. Early heat transfer, coeval with magma emplacement and responsible for the growth of the first andalusite population, occurred by conduction like in every intrusion (Furlong et al., 1991). Presence of fluid flow in the country rocks is documented by the retrograde reaction into sericite from the first andalusite. This implies that early heat transfer occurred not only by conduction but also by fluid flow. However, this fluid-flow-assisted heat transfer was probably not established for too long at a close distance from the pluton because the fluids are often expelled from metamorphic aureoles themselves (Furlong et al., 1991). Indeed, stable isotope data (Harris et al., 1997) indicate the lack of significant hydrothermal alteration in the George pluton. That heat was only temporarily transferred by fluid flow. Growth of the second late to post-kinematic population of andalusites is attributed to the restoration of conduction-dominated heat transfer condition. It is therefore proposed that, during contact metamorphism, a transient hydrothermal episode may be responsible for the splitting of the thermal peak into separate thermal events.

6.4. Static recrystallisation of high-strain fabrics

Static recrystallisation of quartz is pervasive in granites and adjacent country rocks. In order to accumulate the necessary dislocations for the formation of new grains, recrystallisation must have begun dynamically during or shortly after magma emplacement ($\approx$535 Ma). Since static recrystallisation necessitates close to solidus temperatures it is ascribed to the period of cooling of the pluton, and not to the Cape orogeny (280–230 Ma) as previously assumed (Gresse, 1983).

The granites in the Kaaimans inlier and their nearby country rocks have therefore undergone an identical tectono-thermal history marked by an early medium-temperature/high-strain-rate deformation phase followed by a strong static recrystallisation. Microstructures in the Kaaimans inlier close to the granites (Fig. 5a, b and c) attest to a contact metamorphism event coeval with a thrust event. Quartz ribbons, occurring in most lithological types, as well as *C–S* microstructures, are consistent with a top-to-the-north sense of shear. Biotite and Kfs are not usually recrystallised. Ubiquitous recrystallisation of quartz into equigranular polygonal quartz grains (Fig. 5d and e) attest to static conditions. Microscopic observations of the quartz ribbons with a sensitive tint plate indicate a distinctive lattice orientation consistent with a top-to-the-north sense of shear. Similar recovery microstructures have been described by Nicolas and Poirier (1976), also in low strain-rate conditions. Thus most intracrystalline deformation microstructures, such as deformation bands and undulose extinctions, have disappeared leading to a relative microstructural amnesia. However, the lattice preferred orientation in quartz betrays a substantial plastic deformation and the near-solidus fractures in alkali feldspar (Bouchez et al., 1992) attest to solid state deformation in the granites. By contrast, microstructures of the Cape Fold Belt quartzites, in the few tens of metres-wide contact zone with the Kaaimans inlier, indicate low-temperature/high-strain-rate conditions of deformation. This strong strain localisation along the contact zone, after pluton emplacement, further supports the structural decoupling between the two major orogenic domains.

6.5. AMS fabrics and high-strain memory

6.5.1. Origin of the magnetic susceptibility

The George granites display most features of *S*-type granites and are characterised by paramagnetic minerals, such as biotite, muscovite and ilmenite, along

with the paucity of ferromagnetic species (Scheepers, 1995). The magnetic susceptibility magnitudes of the George granites (Maalgaten and Kleinfontein units) and the Rooiklip granite ($20 < K_m < 300$ μSI) are consistent with those of paramagnetic granites ($K_m < 300$ μSI; e.g. Rochette, 1987; Jover et al., 1989). In the Maalgaten and Rooiklip granites, biotite, the most abundant paramagnetic mineral, is presumably at the origin of the bulk rock magnetic susceptibility ($20 < K_m < 270$ μSI). In the Kleinfontein leucogranite, tourmaline also contributes to the magnetic susceptibility ($20 < K_m < 100$ μSI) similarly to the biotite and tourmaline-bearing leucogranites from the Himalayas (Guillot et al., 1993; Rochette et al., 1994). In the Modderkloof granodiorite, by contrast, higher magnetic susceptibilities ($K_m > 450$ μSI), call for the presence of a ferromagnetic contribution.

The paramagnetic volumic susceptibility of the Maalgaten granite has been calculated according to the Curie–Weiss law (see Rochette et al., 1992) using 15 chemical compositions from Potgieter (1950), and measured densities of 2.67 ± 0.02. The calculated K_m (Table 2) range from 60 to 245 μSI, and this is within the range of the Maalgaten samples (Table 1). This confirms that the paramagnetic minerals are the principal contributors to the rock magnetic susceptibility.

The paramagnetic behaviour of the George granites has also been modelled by the quantitative contribution of each mineral to the bulk rock susceptibility: $\Sigma K_{mineral/rock} = \Sigma(V_{mineral/rock} . K_{mineral})$ where $V_{mineral/rock}$ is the mineral volume percentage and $K_{mineral}$ is the mineral intrinsic magnetic susceptibility. The contribution of biotite alone is calculated on the basis of: Mg# (weight ratio) ≈ 0.20 (Krynauw, 1977), yielding an "intrinsic" susceptibility of $K_{Bt} \approx 2100$ μSI; and volume percentage of biotite (V_{Bt}) estimated by point-counting to 2–15% (Potgieter, 1950; Krynauw, 1983). The "intrinsic" susceptibilities and modes of other minerals have been taken respectively from Clark (1997) and Potgieter (1950). The quantitative contribution of biotite to the bulk rock susceptibility is larger than 80% in most samples. The sum of the contributions for the Maalgaten granite ranges from 50 to 500 μSI, which overlays the whole range of measured K_m. Differences are accounted for by errors in the modal counting or minor ferromagnetic contributions such as magnetite in the lattice of biotite crystals (Borradaile and Werner, 1994) or pyrrhotite in the matrix (Rochette, 1987; Jover et al., 1989).

6.5.2. Significance of AMS fabrics

In absence of ferromagnetic species, the anisotropy of magnetic susceptibility results mainly from the magneto-crystalline anisotropy of the ferromagnesian minerals and from their lattice preferred orientation (LPO) in the rock (e.g. Rochette et al., 1992). The 'intrinsic' anisotropy magnitude of a pure biotite crystal is $\approx 32\%$ (Borradaile et al., 1987). The LPO of biotite grains in paramagnetic plutonic rocks results from a variety of mechanisms that occur during magma flow and eventually subsequent plastic deformation overprint.

Magnetic fabrics are very consistent from one station to the other, in the Maalgaten and Rooiklip granites in which biotite is the dominant paramagnetic species. In addition, biotite aggregates display a pre-

Table 2
Low-field magnetic susceptibilities calculated from the whole rock analyses of the Maalgaten granite

Weight%																Mean
Si	70.94	67.11	66.26	67.95	67.74	69.58	66.18	70.82	68.42	67.25	67.73	67.37	67.22	67.23	65.14	67.79
Al	12.53	14.82	15.13	13.38	12.73	12.41	14.16	11.72	13.64	13.04	13.60	13.60	13.82	13.14	15.14	13.52
Fe^{3+}	0.22	1.08	1.10	0.33	0.88	0.43	1.20	0.88	0.91	0.33	1.10	0.77	0.55	1.31	2.06	0.88
Fe^{2+}	0.77	0.23	0.44	0.99	0.77	0.99	0.55	0.55	0.41	1.43	0.44	1.09	1.21	0.45	0.60	0.73
Mg	0.65	0.62	0.98	0.73	1.09	0.58	1.34	0.92	1.09	0.91	0.88	0.90	1.29	1.25	0.75	0.93
Mn	0.04	0.03	0.03	0.42	0.04	0.33	0.05	0.52	0.62	0.52	0.50	0.51	0.73	0.71	0.42	0.37
Ti	0.00	0.15	0.23	0.21	0.30	0.14	0.17	0.00	0.14	0.32	0.27	0.23	0.34	0.33	0.24	0.20
Ca	0.93	0.92	1.86	1.26	1.59	1.20	1.70	1.09	1.07	1.59	0.77	2.14	1.81	1.53	2.63	1.47
Na	5.48	4.63	4.89	4.59	4.43	5.14	5.11	4.01	4.77	5.97	5.85	5.14	3.71	5.21	5.16	4.94
K	4.06	5.96	5.93	5.36	4.84	4.16	5.04	4.04	5.81	4.43	5.25	4.09	3.87	5.35	4.42	4.84
H	2.19	4.44	2.98	3.41	3.28	4.56	3.35	2.92	3.04	3.10	4.93	4.68	5.47	2.62	3.16	3.61
Total	97.81	100.00	99.84	98.62	97.69	99.53	98.85	97.47	99.92	98.88	101.32	100.51	100.02	99.11	99.71	99.29
K_m calc.[a] (10^{-6} SI)	60	99	115	118	118	120	133	147	149	156	157	172	180	195	245	144

[a] K_m calc. = calculated magnetic susceptibility in 10^{-6} SI (after Rochette et al., 1992). Source: Potgieter (1950).

ferred orientation parallel to the stretching lineations marked by the quartzo-feldspathic minerals. Biotite displays both shape- and lattice-preferred orientations and probably controls most of the AMS as attested by the good agreement between the magnetic fabrics and field structures (Fig. 8). In the Kleinfontein leucogranite, the abnormal AMS fabrics are attributed to tourmaline, which has an inverse magnetic fabric with respect to its crystallography (Rochette et al., 1992). In these granites, the magnetic lineation is often at a high angle to the tourmaline–quartz mineral stretching lineation determined in the field (stations #17, #18, #19 and #33 in Fig. 8). In the Modderkloof granodiorite (station #42, Fig. 8), magnetic fabrics are probably controlled by magnetite. Such fabrics, however, appear to mimic the crystalline fabric as suggested by the field and magnetic fabric similarities in orientations in the neighbouring station (#30, Fig. 8). The Modderkloof intrusion is therefore concluded to be emplaced under the same deformation conditions as the Maalgaten granite, and not as a post-tectonic intrusion (Krynauw, 1983). The homogeneous AMS fabrics therefore record a regional scale deformation phase throughout the George granites (Figs. 8 and 9). Taking into account the ubiquitous near-solidus to solid-state microstructures, this deformation was probably imprinted first in the magmatic state, but definitely overprinted ubiquitously in the solid-state. This is also attested by the pervasive *C*–*S* structures (Fig. 10).

As also shown elsewhere by Aranguren et al. (1996), the biotite-controlled magnetic fabrics, can be either parallel to the *S*-planes, parallel to the *C*-planes at increasing strain, or composite, i.e. in between the *C*- and *S*-planes (Fig. 10b). This accounts for local, minute but consistent, discrepancies between the AMS and field structures (Fig. 8). The general obliquity between field foliations (*C*-planes) and magnetic foliations can be observed both on individual stations (Fig. 8) and at the scale of the whole pluton (Figs. 3 and 9). The field foliations dip usually steeper (42°S) than the magnetic foliations (35°S). This obliquity can be used as a shear sense criterion knowing that the magnetic structure is between *C* and *S* (Fig. 10b). It is concluded that the AMS fabrics joint with field foliations provide a top-to-the-north sense of shear and support the thrust tectonic setting. The AMS fabrics mimic the biotite subfabrics acquired before static recrystallisation. These fabrics were not modified by the subsequent thermal metamorphic event and therefore they preserve the emplacement-related deformation fabric.

The positive correlation observed throughout the George pluton, between the anisotropy P_J and the magnetic susceptibility K_m magnitudes (Fig. 7a), could be interpreted as follows: P_J relates to strain magnitude and K_m is a petrological index. Therefore, higher strains would be observed in the less differentiated granites. A detailed analysis of individual stations (Fig. 7b) shows, however, that the magnetic anisotropy varies little with large variations of K_m, except in the late-magmatic shear zone (stations #28–30). Thus the P_J–K_m correlation reflects various amounts of strain that can be ascribed mainly to heterogeneous deformation. Similar P_J–K_m correlations are common in paramagnetic granites (Bouchez, 1997) and are thought to reflect the difference in rheology between felsic and mafic magmas (Bouchez et al., 1992).

7. Conclusion

Distinction between the Saldanian and the Cape tectonic overprints is difficult due to the closeness of metamorphic conditions and to the similarities between kinematic settings. In the Kaaimans inlier, deformation phases can be reduced to less than previously published. The George granite pluton and its country rocks display similar and coeval structures acquired during emplacement. The George pluton is therefore a syntectonic intrusion. Kinematic indicators systematically show a top-to-the-north sense of shear and demonstrate a thrust tectonic setting. In collision orogens, the retrograde part of the *P*–*T*–*t* path occurs fairly shortly after the peak of metamorphism around 535 Ma. Therefore the static metamorphic overprint cannot be coeval with the Cape orogeny (280–230 Ma). The structures observed in the granites, such as near-solidus fractures in alkali feldspar, augen structures and *C*–*S* structures, result from a deformation continuum from magmatic to solid-state conditions. This is consistent with a simple deformation history and a single kinematics. The ubiquitous equigranular polygonal quartz grains show that a pervasive recrystallisation has overprinted the granites and their country rocks. This recrystallisation event has annealed almost all solid-state features resulting in an overall fabric amnesia. The thermal static overprint is the consequence of the thrust tectonics in which deformation proceeds faster than thermal equilibrium can be attained. AMS fabrics are generally thought to record the last deformation increments. In this example, the AMS fabrics, dominantly carried by biotite, mimic the subfabric of this mineral and have not been reset by the static thermal overprint. Therefore, the AMS fabrics record an earlier part of the tectono-metamorphic history. The results presented here provide a template for the interpretation of AMS fabrics in thrust-emplaced granites.

Acknowledgements

This study was supported by Rhodes University

Research Grant No. 36605-500-105 to Eric Ferré and by a scholarship from Paul Sabatier University, France, to Laurent Améglio. We sincerely thank G. Gleizes (Toulouse) and R. Jacob (Rhodes) for their constructive remarks during this work. Pierre Lespinasse (Toulouse) did all the AMS measurements and Alex Mason-Apps helped in the field. Bennet Bongwana and Wilberforce Hashe prepared the 112 thin sections of this study. The people from George are thanked for their very kind assistance in the field. Finally, we thank G. Borradaile and J.L. Bouchez for their thorough reviews.

References

Aranguren, A., Cuevas, J., Tubia, J.M., 1996. Composite magnetic fabrics from *S–C* mylonites. Journal of Structural Geology 18, 863–869.

Archanjo, C.J., Bouchez, J.L., Corsini, M., Vauchez, A., 1994. The Pombal granite pluton: magnetic fabric, emplacement and relationships with the Brasiliano strike-slip setting of NE Brazil (Paraíba State). Journal of Structural Geology 16, 323–335.

Benn, K., Rochette, P., Bouchez, J.L., Hattori, K., 1993. Magnetic susceptibility, magnetic mineralogy and magnetic fabrics in a Late Archean granitoid–gneiss belt. Precambrian Research 63, 59–81.

Benn, K., Horne, R.J., Kontak, D.J., Pignotta, G.S., Evans, N.G., 1997. Syn-Acadian emplacement model for the South Mountain batholith, Meguma Terrane, Nova Scotia: Magnetic fabric and structural analysis. Geological Society of America Bulletin 109, 1279–1293.

Borradaile, G.J., Keeler, W., Alford, C., Sarvas, P., 1987. Anisotropy of magnetic susceptibility of some metamorphic minerals. Physics of the Earth and Planetary Interiors 48, 161–166.

Borradaile, G.J., 1991. Correlation of strain with anisotropy of magnetic susceptibility (AMS). Pure and Applied Geophysics 135, 17–29.

Borradaile, G.J., Werner, T., 1994. Magnetic anisotropy of some phyllosilicates. Tectonophysics 235, 223–248.

Borradaile, G.J., Henry, B., 1997. Tectonic applications of the magnetic susceptibility and its anisotropy. Earth Science Reviews 42, 49–93.

Bouchez, J.L., 1997. Granite is never isotropic: an introduction to AMS studies of granitic rocks. In: Bouchez, J.L., Hutton, D.H.W., Stephens, W.E. (Eds.), Granite: From Segregation of Melt to Emplacement Fabrics. Kluwer Publishing Co, Dordrecht, pp. 95–112.

Bouchez, J.L., Delas, C., Gleizes, G., Nédélec, A., Cuney, M., 1992. Submagmatic microfractures in granites. Geology 20, 35–38.

Bouchez, J.L., Gleizes, G., 1995. Two-stage deformation of the Mont-Louis–Andorra granite pluton (Variscan Pyrenees) inferred from magnetic susceptibility anisotropy. Journal of the Geological Society of London 152, 669–679.

Clark, D.A., 1997. Magnetic petrophysics and magnetic petrology: aids to geological interpretation of magnetic surveys. Journal of Australian Geology and Geophysics 17, 83–103.

de Wit, M.J., Ransome, I.G.D., 1992. Inversion Tectonics of the Cape Fold Belt, Karoo and Cretaceous Basins of Southern Africa. Balkema, Rotterdam.

Dunlevey, J.N., 1988. Evolution of the Saldanhian orogeny and development of the Cape granite suite. South African Journal of Science 84, 565–568.

Dunlevey, J.N., 1992. Pan-African crustal evolution of south-western Africa. Journal of African Earth Sciences 15, 207–216.

Ferré, E., Gleizes, G., Bouchez, J.L., Nnabo, P.N., 1995. Internal fabric and strike-slip emplacement of the Pan-African granite of Solli Hills, northern Nigeria. Tectonics 14, 1205–1219.

Ferré, E., Gleizes, G., Djouadi, M.T., Bouchez, J.L., Ugodulunwa, F.X.O., 1997. Drainage and emplacement of magmas along an inclined transcurrent shear zone: petrophysical evidence from a granite–charnockite pluton (Rahama, Nigeria). In: Bouchez, J.L., Hutton, D.H.W., Stephens, W.E. (Eds.), Granite: From Segregation of Melt to Emplacement Fabrics. Kluwer Publishing Co, Dordrecht, pp. 253–273.

Frey, M., Robinson, D., 1999. Low-grade Metamorphism. Blackwell Science, Oxford, p. 313.

Frimmel, H.E., van Achterbergh, E., 1995. Metamorphism of calc-silicate and associated rocks in the Pan-African Kaaimans Group, Saldania Belt, South Africa. Mineralogy and Petrology 53, 75–102.

Furlong, K.P., Hanson, R.B., Bowers, J.R., 1991. Modeling thermal regimes. In: Kerrick, D.M. (Ed.), Contact Metamorphism, Reviews in Mineralogy, 26. Mineralogical Society of America, pp. 437–505.

Gresse, P.G., 1983. Lithostratigraphy and structures of the Kaaimans Group. Geological Society of South Africa Special Publication 12, 7–19.

Gresse, P.G., Theron, J.N., Fitch, F.J., Miller, J.A., 1992. Tectonic inversion and radiometric resetting of the basement in the Cape Fold Belt. In: de Wit, M.J., Ransome, I.G.D. (Eds.), Inversion tectonics of the Cape Fold Belt, Karoo and Cretaceous Basins of Southern Africa. Balkema, Rotterdam, pp. 217–228.

Gresse, P.G., Scheepers, R., 1993. Neoproterozoic to Cambrian (Namibian) rocks of South Africa: a geochronological and geotectonic review. Journal of African Earth Sciences 16, 375–393.

Guillot, S., Pêcher, A., Rochette, P., Le Fort, P., 1993. The emplacement of the Manaslu granite of central Nepal: field and magnetic susceptibility constraints. In: Treloar, P.J., Searle, M.P. (Eds.), Himalayan Tectonics, The Geological Society Special Publication, 74, pp. 413–428.

Harris, C., Faure, K., Diamond, R.E., Scheepers, R., 1997. Oxygen and hydrogen isotope geochemistry of S- and I-type granitoids: the Cape Granite suite, South Africa. Chemical Geology (Isotope Geoscience Section) 143, 95–114.

Hartnady, C., Joubert, P., Stowe, C., 1985. Proterozoic crustal evolution in southwestern Africa. Episodes 8, 236–244.

Hälbich, I.W., Cornell, D.H., 1983. Metamorphic history of the Cape Fold belt. Geological Society of South Africa Special Publication 12, 131–148.

Jelinek, V., 1978. Statistical processing of anisotropy of magnetic susceptibility measured on groups of specimen. Studia Geophyzika et Geodetika 22, 50–62.

Jover, O., Rochette, P., Lorand, J.P., Maeder, M., Bouchez, J.L., 1989. Magnetic mineralogy of some granites from the French Massif Central: origin of their low field susceptibility. Physics of the Earth and Planetary Interiors 55, 79–92.

Kretz, R., 1983. Symbols for rock-forming minerals. American Mineralogist 68, 277–279.

Krynauw, J.R., 1977. The George granite pluton and its relationship to the Kaaimans formation. MSc thesis, Stellenbosch University.

Krynauw, J.R., Gresse, P.G., 1980. The Kaaimans Group in the George area, Cape province: a model for the origin of deformation and metamorphism in the Southern Cape Fold Belt. Transactions of the Geological Society of South Africa 83, 23–38.

Krynauw, J.R., 1983. Granite intrusion and metamorphism in the Kaaimans Group. Geological Society of South Africa Special Publication 12, 21–32.

Nicolas, A., Poirier, J.P., 1976. Crystalline plasticity and solid state

flow in metamorphic rocks. Selected topics in Geological Sciences. John Wiley & Sons, London, p. 444.

Noltimier, H.C., 1971. Determining magnetic anisotropy of rocks with a spinner magnetometer giving in-phase and quadrature data output. Journal of Geophysical Research Solid Earth 76, 4849–4854.

Nyman, M.W., Law, R.D., Morgan, S.S., 1995. Conditions of contact metamorphism, Papoose Flat Pluton, eastern California, USA: implications for cooling and strain histories. Journal of Metamorphic Geology 13, 627–643.

Passchier, C.W., Trouw, R.A.J., 1996. Microtectonics. Springer–Verlag, Berlin.

Paterson, S.R., Vernon, R.H., 1995. Bursting the bubble of ballooning plutons: A return to nested diapirs emplaced by multiple processes. Geological Society of America Bulletin 107, 1356–1380.

Potgieter, C.T., 1950. The structure and petrology of the George granite plutons and the invaded pre-Cape sedimentary rocks. Annals of the University of Stellenbosch section A 26, 323–412.

Riller, U., Cruden, A.R., Schwerdtner, W.M., 1996. Magnetic fabric and microstructural evidence for a tectono-thermal overprint of the early Proterozoic Murray pluton, central Ontario, Canada. Journal of Structural Geology 18, 1005–1016.

Rochette, P., 1987. Magnetic susceptibility of the rock matrix related to magnetic fabric studies. Journal of Structural Geology 9, 1015–1020.

Rochette, P., Jackson, M., Aubourg, C., 1992. Rock magnetism and the interpretation of anisotropy of magnetic susceptibility. Reviews of Geophysics 30, 209–226.

Rochette, P., Scaillet, B., Guillot, S., Le Fort, P., Pêcher, A., 1994. Magnetic properties of the High Himalayan leucogranites: Structural implications. Earth and Planetary Science Letters 126, 217–234.

Saint Blanquat, M. de, Tikoff, B., 1997. Development of magmatic to solid-state fabrics during syntectonic emplacement of the Mono Creek granite, Sierra Nevada Batholith. In: Bouchez, J.L., Hutton, D.H.W., Stephens, W.E. (Eds.), Granite: From Segregation of Melt to Emplacement Fabrics. Kluwer Publishing Co, Dordrecht, pp. 231–252.

Scheepers, R., 1995. Geology, geochemistry and petrogenesis of Late Precambrian S-, I- and I-type granitoids in the Saldania belt, Western Cape Province, South Africa. Journal of African Earth Sciences 21, 35–58.

Söhnge, A.P.G., Hälbich, I.W., 1983. Geodynamics of the Cape Fold Belt. Geological Society of South Africa Special Publication 12, 184.

Thomas, R.J., von Veh, M.W., McCourt, S., 1993. The tectonic evolution of southern Africa: an overview. Journal of African Earth Sciences 16, 5–24.